Utilization of a Syn to Anti Rearrangement for the Construction of a Centrosymmetric, Covalently Linked Cross Section That Would Direct Parallel Strandedness in a Double-Helical Polynucleotide

Nelson J. Leonard,*,† Balkrishen Bhat, Scott R. Wilson, and Kenneth A. Cruickshank

Contribution from the Roger Adams Laboratory, School of Chemical Sciences, University of Illinois, 1209 West California Street, Urbana, Illinois 61801-3731. *Received June 7, 1990*

Abstract: X-ray crystal structures have been determined and compared for fluorescent 1,3,4,6-tetraazapentalenes that are syn and anti disubstituted with pyrimidinone rings or with a combination of pyrimidinone and pyridine rings. Syn-disubstituted tetraazapentalenes were synthesized by a three-step sequence from 1-ethylcytosine or O-protected cytidine (also O-protected adenosine), chloroketene diethyl acetal, and either 2-aminopyridine or another cytosine or cytidine unit. The final step was an oxidative cyclization by means of an I^{III} compound. Anti-disubstituted tetraazapentalenes bearing terminal pyrimidinone rings or pyrimidinone and pyridine rings were obtained from the corresponding syn compounds by treatment with ammonia or sodium methoxide in methanol. The most likely pathway for the facile syn to anti conversion involves nucleophilic attack on carbonyl by NH_3 or CH_3O^-, bond breaking at the new sp^3 center in the direction of an amide/imidazolide or carbamate/imidazolide intermediate, and bond rotation and reclosure at the less hindered imidazolide nitrogen with formal loss of NH_3 or CH_3O^-. The anti tetracyclic ring system based on two cytidine units attached to the 1,3,4,6-tetraazapentalene central moiety provides a covalently linked cross section that is a model for base pairing in a double-helical polynucleotide having *parallel* rather than antiparallel strands.

The process of constructing compounds of biological interest based on a central 1,3,4,6-tetraazapentalene ring system has uncovered a reaction involving pyrimidinone ring opening and reclosure.[1] We have applied this reaction to the synthesis of a covalently linked cross section that would fix a double-helical polynucleotide in parallel rather than antiparallel strands.[2] We now describe the details of this chemistry and outline some potential applications. Developments are presented in logical, although not necessarily chronological, order so as to simplify the discussion. Single-crystal X-ray analyses of the syn precursors and anti products provide the structural assignments and suggest the probable basis for the rearrangement.

Syn- and anti-dipyrido-substituted 1,3,4,6-tetraazapentalenes (**1a**,**b**) have been prepared recently by separate oxidative cyclization routes,[3-5] and their spectroscopic, photophysical, and photochemical properties nave been compared.[6] X-ray structure determinations showed these isomers to be planar and the bond lengths in the external rings to be indicative of alternation in multiplicity. The synthesis that led to the syn isomer, pyrido[1″,2″:1′,2′]imidazo[4′,5′:4,5]imidazo[1,2-*a*]pyridine (**1a**), which consisted of two steps from 2-aminopyridine, served as a model for the construction of covalently linked DNA/RNA cross sections representative of purine–pyrimidine, purine–purine, and pyrimidine–pyrimidine duplexes.[7-9] The synthetic methodology has been applied to hybrid examples that are monopyrido-substituted 1,3,4,6-tetraazapentalenes.

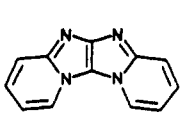

1a

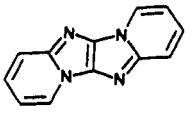

1b

N^6-(1-Ethoxy-2-chloroethylidene)-2′,3′,5′-tri-*O*-acetyladenosine (**2a**)[7,9,10] was used to make the product that had additional purine substitution and N^4-(1-ethoxy-2-chloroethylidene)-2′,3′,5′-tri-*O*-acetylcytidine (**3a**),[8-10] for the product that had additional pyrimidinone substitution. Compounds **2a** and **3a** were heated separately with 2-aminopyridine to afford the intermediates **4a**, mp 194 °C, and **5a**, mp 166–167 °C. The yields were 45% and 21%, respectively, but, based on unrecovered starting material, were higher. The structure of **4a** was indicated by low- and high-resolution FAB mass spectrometric data and by the NMR chemical shift of the original 2-proton on the purine nucleus in

Scheme I

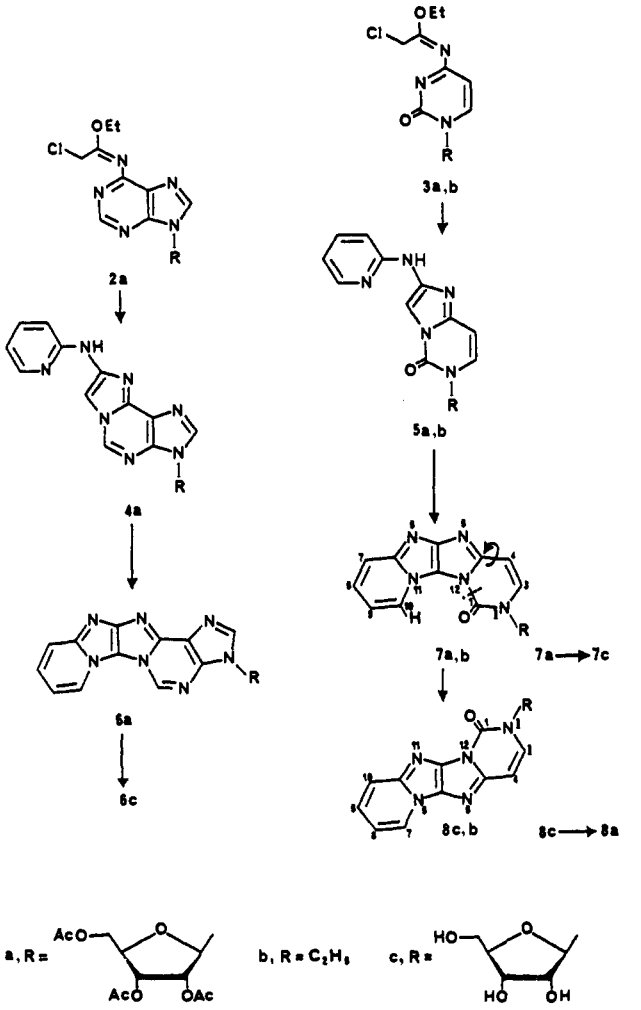

† Fogarty Scholar-in-Residence, 1989–1990, National Institutes of Health, U.S. Public Health Service, Bethesda, MD 20892.

(1) Bhat, B.; Cruickshank, K. A.; Leonard, N. J. *J. Org. Chem.* **1989**, *54*, 2028.

0002-7863/91/1513-1398$02.50/0

Table I. Crystallographic and Intensity Data Collection Parameters for **7b**, **8b**, **14**, and **15**[e]

	7b[a]	**8b**[b]	**14**[c]	**15**[d]
formula	$C_{13}H_{11}N_5O$	$C_{13}H_{11}N_5O$	$C_{14}H_{14}N_6O_2$	$^1/_2$ ($C_{14}H_{14}N_6O_2$)
form wt, amu	253.26	253.26	298.30	$^1/_2$ (298.30)
crystal class	monoclinic	monoclinic	monoclinic	monoclinic
space group	$P2_1/c$ (C^5_h)	$P2_1/c$ (C^5_h)	$P2_1/c$ (C^5_h)	$P2_1/c$ (C^5h)
dimensions, mm	0.2 × 0.3 × 0.8	0.1 × 0.1 × 0.5	0.1 × 0.1 × 0.7	0.3 × 0.3 × 0.6
a, Å	7.862 (3)	7.048 (5)	13.092 (5)	4.4540 (4)
b, Å	12.012 (5)	12.350 (8)	13.240 (3)	11.2235 (11)
c, Å	12.406 (4)	13.327 (8)	7.890 (5)	13.4663 (15)
β, deg	96.78 (3)	97.84 (5)	102.37 (4)	91.128 (4)
V, Å^3	1163.5 (7)	1149 (1)	1336 (2)	673.0 (2)
Z	4	4	4	4 (2)
ρ(calcd), g/cm^3	1.446	1.464	1.483	1.472
radiation, λ, Å	Mo Kᾱ, 0.71073	Mo Kᾱ, 0.71073	Mo Kᾱ, 0.71073	Mo Kᾱ, 0.71073
diffractometer	Syntex $P2_1$	Syntex $P2_1$	Enraf-Nonius CAD4	Syntex $P2_1$
octants, scan mode	$\pm h,+k,+l$, $\omega/2\theta$	$\pm h,+k,+l$, $\omega/2\theta$	$\pm h,-k,-l$, $\omega/2\theta$	$+h,+k,\pm l$, $\omega/2\theta$
μ, cm^{-1}	0.92	0.93	0.99	0.98
2θ range, deg	3–46	3–40	2–40	3–50
no. of intensities measd	1880	1853	3338	2176
no. of unique intensities	1576	1615	2905	1549
no. of obsd reflections	1072	979	1270	1295
R	0.048	0.054	0.046	0.037
R_w	0.054	0.050	0.047	0.053
no. of variables	174	174	242	129
p	0.020	0.020	0.020	0.001

[a] 2-Ethylpyrido[1″,2″:1′,2′]imidazo[4′,5′:4,5]imidazo[1,2-*c*]pyrimidin-1-one. [b] 2-Ethylpyrido[2″,1″:2′,3′]imidazo[4′,5′:4,5]imidazo[1,2-*c*]pyrimidin-1-one. [c] 2,9-Diethylpyrimido[1″,6″:1′,2′]imidazo[4′,5′:4,5]imidazo[1,2-*c*]pyrimidine-1,10-dione. [d] 2,8-Diethylpyrimido[1″,6″:3′,2′]imidazo[4′,5′:4,5]imidazo[1,2-*c*]pyrimidine-1,7-dione. [e] All compounds were crystallized from MeOH.

2a, which moved to lower field in **4a** by 0.6 ppm and was thus diagnostic of ring closure on the purine side.[7,10] Oxidative cyclization of **4a** with iodobenzene diacetate ((diacetoxyiodo)-benzene) in trifluoroethanol[3,4,7-9] yielded (55%) 3-(2,3,5-tri-*O*-acetyl-β-D-ribofuranosyl)-3*H*-pyrido[1″,2″:1′,2′]imidazo[2,1-*i*]-purine (**6a**), mp 227–228 °C. The structure was confirmed by low- and high-resolution FAB mass spectral and ^{1}H NMR spectral data. Evidence of the second ring closure, with the formation of the pentacyclic heteroaromatic system, was provided by the further downfield shift (0.6 ppm) of the proton in the pyrimidine ring. The *O*-acetyl protecting groups in **6a** were removed by methanolic ammonia at 30 °C to yield (75%) 3-(β-D-ribofuranosyl)-3*H*-pyrido[1″,2″:1′,2′]imidazo[4′,5′:4,5]imidazo[2,1-*i*]purine (**6c**), mp 270–271 °C. The composition of **6c** was confirmed by low- and high-resolution FAB mass spectra, and the identity of the N-pentacyclic ring system in **6a** and **6c** was shown by the nearly identical chemical shifts in the ^{1}H NMR for the aromatic protons and by the matching UV spectra in the region 238–250 nm for **6a** and **6c**.

In the pyrimidinone series, the occurrence of the first ring closure, **3a** → **5a**, with the creation of the etheno bridge on the cytidine side rather than the pyridine side of the system, was indicated by the usual spectroscopic criteria and by the marked downfield shift (0.93 ppm) of the original 5-H of the cytidine moiety, upfield shift (0.15 ppm) of the original 6-H, and corresponding net decrease in chemical shift difference between the pyrimidine ring protons.[8-10] Oxidative cyclization of **5a** yielded (50%) the tetracyclic N-heteroaromatic ring structure **7a**, mp 140–143 °C, confirmed by microanalytical, low- and high-resolution FAB mass spectral, and ^{1}H NMR spectral data. However, when removal of the *O*-acetyl protecting groups in **7a** was attempted with methanolic ammonia at 30 °C, while the colorless solid that resulted exhibited a molecular ion at m/z 358 (MH^+) in the FAB mass spectrum, satisfactory for the O-deprotected compound, the ^{1}H NMR spectrum indicated the presence of two ribonucleosides of very similar structure.

Reacetylation of this product with Ac_2O/pyridine gave a mixture of two compounds that could be separated more readily by thin-layer silica gel chromatography, 10% MeOH in $CHCl_3$ as solvent. The compound with R_f value 0.52 corresponded to **7a** while the faster moving component, R_f 0.67, showed the same molecular ion, m/z 484 (MH^+), and one marked difference among the ^{1}H NMR signals. The resonance at δ 9.09 for **7a**, which corresponded to the proton at C10, deshielded by the paramagnetic anisotropy[11] of the proximal carbonyl group in the bay region, was shifted upfield by 0.35 ppm to δ 8.74 in the second compound.

We examined the behavior of a simplified version of **7a**, namely **7b**, in order to exclude possible complications resulting from the presence of the ribofuranosyl moiety. For the synthesis of **7b**, 1-ethylcytosine[12] was first treated with chloroketene diethyl acetal in acetonitrile at 30 °C for 20 h to give **3b** in 80% yield. This compound, N^4-(1-ethoxy-2-chloroethylidene)-1-ethylcytosine (**3b**), was condensed with 2-aminopyridine to give the precursor **5b** in 30% yield. Oxidative cyclization of **5b** with iodobenzene diacetate in trifluoroethanol yielded (58%) 2-ethylpyrido[1″,2″:1′,2′]-imidazo[4′,5′:4,5]imidazo[1,2-*c*]pyrimidin-1-one (**7b**): $C_{13}H_{11}N_5O$, mp 261–262 °C, FTIR 1680.2 cm^{-1}. The longest wavelength maximum in the ultraviolet spectrum is at 364 nm (MeOH), and the compound shows a fluorescence maximum at 393 nm when irradiated at 350 nm (absolute EtOH).

When compound **7b** was treated with ammonia in methanol at room temperature for 24 h or with 0.4 M $NaOCH_3$ in methanol during a shorter time period, an isomeric product resulted that had greater mobility in TLC on silica gel; R_f 0.62 vs 0.55, 10% MeOH in $CHCl_3$ as solvent. For the new $C_{13}H_{11}N_5O$ product, mp 279–280 °C, FTIR 1686 cm^{-1}, the longest wavelength maximum in the ultraviolet spectrum is at 374 nm (MeOH), and the fluorescence emission maximum is at 418 nm for excitation at 350 nm (absolute EtOH). The major difference observed in the ^{1}H NMR spectra of **7b** and its isomer was the upfield shift, by 0.39 ppm, of the proton magnetic resonance from δ 9.12 in **7b**

(2) Bhat, B.; Leonard, N. J. *J. Org. Chem.* **1989**, *54*, 2030.
(3) Cruickshank, K. A.; Sumoto, K.; Leonard, N. J. *Tetrahedron Lett.* **1985**, *26*, 2723.
(4) Pereira, D. E.; Clauson, G. L.; Leonard, N. J. *Tetrahedron* **1987**, *43*, 4931.
(5) Groziak, M. P.; Wilson, S. R.; Clauson, G. L.; Leonard, N. J. *J. Am. Chem. Soc.* **1986**, *108*, 8002.
(6) Halpern, A. M.; Ruggles, C. J.; Zhang, X.-k.; Groziak, M. P.; Leonard, N. J. *J. Phys. Chem.* **1987**, *91*, 1366.
(7) Devadas, B.; Leonard, N. J. *J. Am. Chem. Soc.* **1986**, *108*, 5012.
(8) Leonard, N. J.; Devadas, B. *J. Am. Chem. Soc.* **1987**, *109*, 623.
(9) Devadas, B.; Leonard, N. J. *J. Am. Chem. Soc.* **1990**, *112*, 3125.
(10) Leonard, N. J.; Cruickshank, K. A. *J. Org. Chem.* **1985**, *50*, 2480.
(11) Vul'fson, S. G.; Nikolaev, V. F.; Vereshchagin, A. N. *Bull. Acad. Sci. SSSR, Div. Chem. Sci.* **1985**, *34*, 732.
(12) Helfer, D. L., II; Hosmane, R. S.; Leonard, N. J. *J. Org. Chem.* **1981**, *46*, 4803.

Table II. Selected Bond Lengths and Angles for **7b**

bond	length, Å (esd)	bond	length, Å (esd)
O-C1	1.214 (4)	C8-C9	1.401 (6)
C1-N2	1.367 (4)	C9-C10	1.347 (5)
N2-C3	1.375 (4)	C10-N11	1.374 (4)
C3-C4	1.333 (5)	N11-C6a	1.420 (4)
C4-C4a	1.415 (5)	N11-C11a	1.367 (4)
C4a-N5	1.321 (4)	C5a-C11a	1.356 (4)
N5-C5a	1.385 (4)	C11a-N12	1.370 (4)
C5a-N6	1.365 (4)	N12-C1	1.389 (4)
N6-C6a	1.333 (4)	N12-C4a	1.423 (4)
C6a-C7	1.413 (5)	N2-C13	1.465 (4)
C7-C8	1.355 (5)	C13-C14	1.493 (5)
atoms	angle, deg (esd)	atoms	angle, deg (esd)
O-C1-N2	125.3 (3)	N11-C6a-N6	113.8 (3)
C1-N2-C3	122.7 (3)	N11-C6a-C7	116.1 (3)
C1-N2-C13	117.9 (3)	N11-C11a-C5a	108.1 (3)
C3-N2-C13	119.4 (3)	N11-C11a-N12	144.1 (3)
N2-C3-C4	123.5 (3)	C11a-N11-C6a	102.8 (2)
C3-C4-C4a	118.7 (3)	C11a-C5a-N5	111.9 (3)
C4-C4a-N5	131.5 (3)	C11a-C5a-N6	112.6 (3)
C4a-N5-C5a	103.5 (3)	C11a-N12-C1	130.2 (3)
N5-C5a-N6	135.6 (3)	C11a-N12-C4a	103.9 (2)
C5a-N6-C6a	102.7 (3)	N12-C1-O	121.1 (3)
N6-C6a-C7	130.1 (3)	N12-C1-N2	113.7 (3)
C6a-C7-C8	119.8 (3)	N12-C4a-C4	115.5 (3)
C7-C8-C9	121.5 (3)	N12-C4a-N5	113.0 (3)
C8-C9-C10	121.1 (3)	N12-C11a-C5a	107.7 (3)
C9-C10-N11	117.9 (3)	C1-N12-C4a	125.8 (2)
C10-N11-C6a	123.6 (3)	N2-C13-C14	112.3 (3)
C10-N11-C11a	133.6 (3)		

Table III. Selected Bond Lengths and Angles for **8b**

bond	length, Å (esd)	bond	length, Å (esd)
O-C1	1.206 (5)	C8-C9	1.407 (7)
C1-N2	1.381 (5)	C9-C10	1.361 (6)
N2-C3	1.378 (5)	C10-C10a	1.405 (6)
C3-C4	1.339 (6)	C10a-N11	1.346 (5)
C4-C4a	1.410 (6)	N11-C11a	1.364 (5)
C4a-N5	1.330 (5)	C5a-C11a	1.342 (6)
N5-C5a	1.372 (5)	C11a-N12	1.399 (5)
C5a-N6	1.369 (5)	N12-C1	1.387 (5)
N6-C7	1.371 (5)	N12-C4a	1.420 (5)
N6-C10a	1.413 (5)	N2-C13	1.476 (5)
C7-C8	1.342 (6)	C13-C14	1.505 (6)
atoms	angle, deg (esd)	atoms	angle, deg (esd)
O-C1-N2	124.8 (4)	C10a-N6-C5a	104.2 (3)
C1-N2-C3	123.8 (3)	C10a-N6-C7	123.0 (3)
C1-N2-C13	116.7 (3)	N11-C10a-N6	113.3 (3)
C3-N2-C13	119.5 (3)	N11-C11a-N12	140.1 (3)
N2-C3-C4	122.1 (4)	N11-C11a-C5a	115.1 (3)
C3-C4-C4a	119.4 (4)	C11a-N12-C1	129.5 (3)
C4-C4a-N5	130.6 (4)	C11a-N12-C4a	104.2 (3)
C4a-N5-C5a	101.4 (3)	C11a-C5a-N5	115.9 (4)
N5-C5a-N6	137.8 (4)	C11a-C5a-N6	106.2 (3)
C5a-N6-C7	132.8 (3)	N12-C1-O	122.6 (3)
N6-C7-C8	118.6 (4)	N12-C1-N2	112.6 (3)
C7-C8-C9	121.1 (4)	N12-C4a-C4	115.7 (4)
C8-C9-C10	120.5 (4)	N12-C4a-N5	113.7 (3)
C9-C10-C10a	120.1 (4)	N12-C11a-C5a	104.8 (3)
C10-C10a-N6	116.7 (4)	C1-N12-C4a	126.3 (3)
C10-C10a-N11	130.0 (4)	N2-C13-C14	112.9 (4)
C10a-N11-C11a	101.2 (3)		

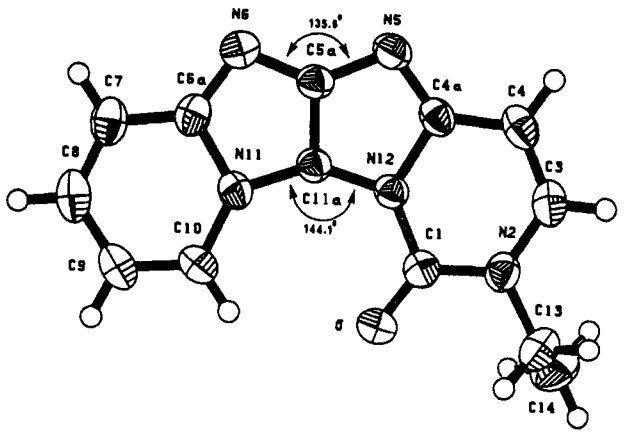

Figure 1. Single ORTEP drawing of 2-ethylpyrido[1″,2″:1′,2′]imidazo-[4′,5′:4,5]imidazo[1,2-*c*]pyrimidin-1-one (**7b**), with the atom numbering, based on the X-ray crystal structure.

to δ 8.73 in the isomer, similar to the change recorded for the ribosyl-substituted pair of isomers.

The significant differences in the ^{1}H NMR spectra and in the ultraviolet absorption and fluorescence emission spectra of **7b** and its isomer were suggestive of the conversion of the syn to an anti product, i.e., **7b** to **8b**, under the basic conditions described. The structures of **7b** and **8b** were established conclusively by X-ray analysis.

The crystallographic and intensity data for **7b** and the other three compounds examined by single-crystal X-ray analysis are shown in Table I, and the bond lengths and angles for **7b** are provided in Table II. The bonds in the pyrido-1,3,4,6-tetraazapentalene portion of the molecule are all within 0.01 Å of the corresponding distances obtained in the X-ray analysis of pyrido[1″,2″:1′,2′]imidazo[4′,5′:4,5]imidazo[1,2-*a*]pyridine (**1a**).[5] This includes the feature that the carbon–carbon bonds in the pyrido periphery are of alternating length, 1.347–1.355 and 1.401–1.413 Å, a finding indicative of the nonzwitterionic predominating resonance form. Figure 1 provides a single ORTEP drawing representative of the crystal structure of compound **7b**. We indicated in our communication[1] that this syn isomer (**7b**) has a slightly warped ring structure. In the crystal, there exist no strong intermolecular contacts and no strong hydrogen bonding. There is one weak intermolecular contact, H3···N5, and there is one weak intramolecular contact, H10···O.

The anti isomer **8b** obtained from **7b** under basic conditions has an essentially planar ring structure. The bond lengths and angles for **8b** are given in Table III. In the pyrido-1,3,4,6-tetraazapentalene portion of the molecule, they are similar to the values obtained in the X-ray analysis of pyrido[2″,1″:2′3′]-imidazo[4′,5′:4,5]imidazo[1,2-*a*]pyridine (**1b**).[5] The carbon–carbon bonds in the pyrido periphery are of alternating length, 1.342–1.361 and 1.405–1.407 Å, as in its isomer **7b**. In the crystal, there exist no strong intermolecular contacts and no specific hydrogen interactions. The chief difference in the interatomic angles in the structures of the syn (**7b**) and anti (**8b**) isomers lies in the spreading of external angle N11–C11a–N12 in the bay region of the syn compound to 144.1 (3)°. The opposing angle, N5–C5a–N6, is 135.6 (3)°. For the anti compound, the external angles central to the 1,3,4,6-tetraazapentalene ring system are 140.1 (3)° for N11–C11a–N12 and 137.8 (4)° for N5–C5a–N6 (Figure 2). As we illustrated in our communication,[1] the anti isomer (**8b**) has an essentially planar structure.

The warped, slightly spread syn ring system in **7b** finds a plausible conversion pathway to the planar, less strained anti ring system in **8b** via nucleophilic attack at the carbonyl by CH_3O^- or NH_3, bond breaking at the new sp^3 center in the direction of a carbamate/imidazolide or amide/imidazolide intermediate, rotation about the original C4–C4a bond, and reclosure at the less hindered imidazolide nitrogen (originally N5), with formal loss of CH_3O^- or NH_3. There is analogy for such pyrimidinone ring opening and reclosure in an energetically favored direction in certain bicyclic[13,14] and tricyclic[15] systems. The conversion that we have observed is most welcome since it provides a reliable route to heretofore unavailable *anti*-disubstituted-1,3,4,6-tetraazapentalenes in which at least one of the terminal rings is of the pyrimidinone type.

(13) Ivanesics, C.; Zbiral, E. *Justus Liebigs Ann. Chem.* **1975**, 1934.
(14) Ueda, T.; Fox, J. J. *J. Org. Chem.* **1964**, *29*, 1762.
(15) Itaya, T.; Mizutani, A. *Tetrahedron Lett.* **1985**, *26*, 347.

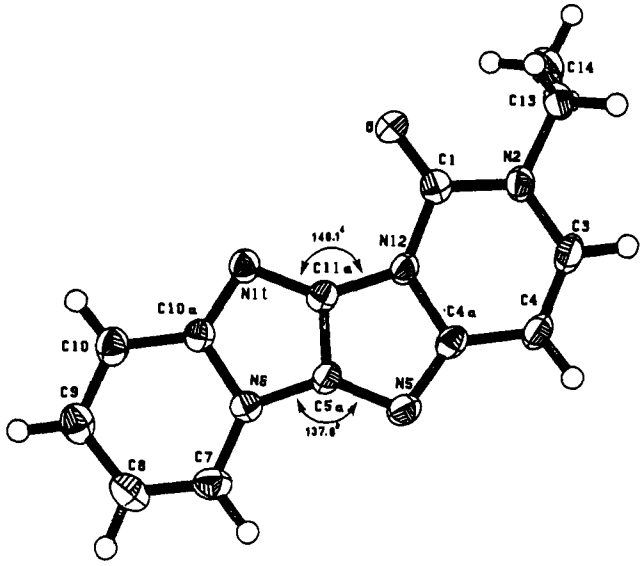

Figure 2. Single ORTEP drawing of 2-ethylpyrido[2″,1″:2′,3′]imidazo-[4′,5′:4,5]imidazo[1,2-*c*]pyrimidin-1-one (**8b**), with the atom numbering, based on the X-ray crystal structure.

In the case of the ribosyl-substituted compounds, O-deprotection of **7a** by a more selective treatment, i.e., with 0.2 M *tert*-butylamine in methanol at −10 to −5 °C for 3 h,[9] preserved the syn ring system and yielded (79%) 2-(β-D-ribofuranosyl)pyrido-[1″,2″:1′,2′]imidazo[4′,5′:4,5]imidazo[1,2-*c*]pyrimidin-1-one (**7c**). This product retained the low-field signal (δ 9.13) of the 10-H in the vicinity of the carbonyl oxygen in the bay region. The electronic spectroscopic values, UV absorption at λ_{max} = 364 nm (MeOH) (longest wavelength) and fluorescence emission at λ_{max}^{em} = 393 nm for λ_{max}^{ex} 350 nm (absolute EtOH), were identical with those of **7b**, of X-ray-established structure. Conversion of **7a** to the anti product, 2-(β-D-ribofuranosyl)pyrido[2″,1″:2′,3′]-imidazo[4′,5′:4,5]imidazo[1,2-*c*]pyrimidin-1-one (**8c**), was effected with ammonia in methanol at room temperature or, preferably, with 0.4 M $NaOCH_3$ in methanol (89% yield). The ^1H NMR signal at δ 9.13 in **7c** was shifted upfield in **8c**, and the electronic absorption maximum appeared at 374 nm (MeOH) (longest wavelength), the fluorescence emission maximum, at 419 nm, with a high fluorescence yield (Φ = 0.74). The reacetylated derivative **8a** from **8c** had similar spectra and an R_f value of 0.67 (see above) in 10% MeOH/$CHCl_3$.

Further applications are suggested by the chemistry that has been described so far. For example, since structure **6c** represents an extended 1,N^6-ethenoadenosine system,[16] the corresponding fluorescent 5′-di- and triphosphates may be interesting candidates, like εADP and εATP, for the examination of coenzyme–enzyme interactions.[17] The fluorescence of **8c** can be similarly exploited in the cytidine series. Another example is based upon one (**9**)

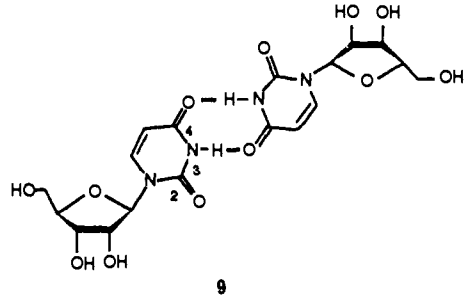

9

among the hypothetical hydrogen-bonding patterns between two uridine moieties that have been considered.[18] Such base pairing

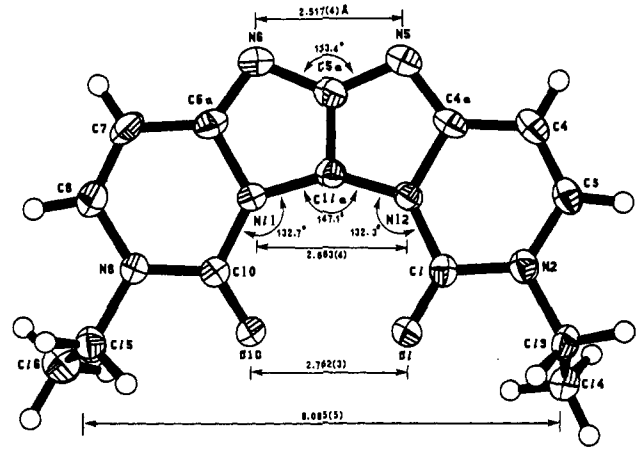

Figure 3. Single ORTEP drawing of 2,9-diethylpyrimido[1″,6″:1′,2′]-imidazo[4′,5′:4,5]imidazo[1,2-*c*]pyrimidine-1,10-dione (**14**), with the atom numbering, based on the X-ray crystal structure.

Scheme II

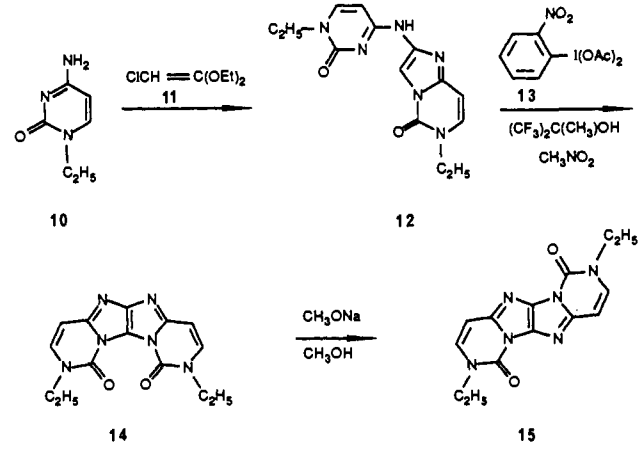

would lead, in a polynucleotide double helix, to parallel strands. A covalently linked cross section representative of base pairing in a double-helical polynucleotide having parallel strands could be obtained by formally substituting a central 1,3,4,6-tetraazapentalene system for the eight-membered, doubly hydrogen bonded ring in **9**.

First, a simplified version was constructed (Scheme II) based on two 1-ethylcytosine (**10**)[12] units. The conditions for the condensation of 1-ethylcytosine with chloroketene diethyl acetal (**11**) were more strenuous than those used to prepare **3b** or the immediate precursor of **1a**.[3] A mixture of **10** and **11** in 2:1 proportion was heated in anhydrous DMF/benzene (1:1) at 90 °C for 24 h (see Experimental Section) to obtain compound **12** (20% yield) in the presence of side products. Oxidative cyclization of **12** required 2-nitro(diacetoxyiodo)benzene (2-nitroiodobenzene diacetate, **13**) in a solvent consisting of 1,1,1,3,3,3-hexafluoro-2-methyl-2-propanol and nitromethane.[7-9] Isolation and purification of the $C_{14}H_{14}N_6O_2$ product was accomplished by flash chromatography on silica gel, elution with 3–5% MeOH in $CHCl_3$, followed by recrystallization from methanol (54% yield). The structure was established as 2,9-diethylpyrimido[1″,6″:1′,2′]-imidazo[4′,5′:4,5]imidazo[1,2-*c*]pyrimidine-1,10(2*H*,9*H*)-dione (**14**) by ^1H NMR spectroscopy, which indicated symmetry in the molecule, FAB mass spectrometry, elemental analysis, and finally X-ray crystallography (Figure 3). The electronic spectra showed UV absorption at λ_{max} = 351 nm (MeOH) (longest wavelength) and fluorescence emission at λ_{max}^{em} 389 and 410 (sh) nm for λ_{max}^{ex}

(16) Leonard, N. J. *CRC Crit. Rev. Biochem.* **1984**, *15*, 125.
(17) For example: Secrist, J. A., III; Barrio, J. R.; Leonard, N. J.; Weber, G. *Biochemistry* **1972**, *11*, 3499.

(18) (a) Saenger, W. *Principles of Nucleic Acid Structure*; Springer-Verlag: New York, 1983; pp 120–121, Figure 6-1. All possible base pairings for A, G, U (T), and C involving at least two (cyclic) hydrogen bonds are considered. (b) Arnott, S. *Prog. Biophys. Mol. Biol.* **1970**, *21*, 265. (c) Gmeiner, W. H.; Poulter, C. D. *J. Am. Chem. Soc.* **1988**, *110*, 7640.

Table IV. Selected Bond Lengths and Angles for **14**

bond	length, Å (esd)	bond	length, Å (esd)
O-C1	1.201 (4)	O10-C10	1.201 (4)
C1-N2	1.380 (4)	C10-N11	1.406 (4)
N2-C3	1.381 (5)	N11-C6a	1.425 (4)
C3-C4	1.331 (6)	N11-C11a	1.394 (4)
C4-C4a	1.410 (5)	C5a-C11a	1.356 (5)
C4a-N5	1.318 (5)	C11a-N12	1.381 (4)
N5-C5a	1.370 (5)	N12-C1	1.404 (4)
C5a-N6	1.370 (5)	N12-C4a	1.424 (4)
N6-C6a	1.313 (5)	N2-C13	1.468 (5)
C6a-C7	1.414 (5)	N9-C15	1.477 (5)
C7-C8	1.327 (6)	C13-C14	1.507 (6)
C8-N9	1.376 (5)	C15-C16	1.484 (7)
N9-C10	1.369 (5)		

atoms	angle, deg (esd)	atoms	angle, deg (esd)
O-C1-N2	123.7 (3)	C10-N11-C6a	123.5 (3)
C1-N2-C3	124.4 (3)	C10-N11-C11a	132.7 (3)
C1-N2-C13	116.0 (3)	N11-C6a-N6	113.6 (3)
C3-N2-C13	119.5 (3)	N11-C6a-C7	116.6 (3)
N2-C3-C4	121.5 (4)	N11-C11a-C5a	106.2 (3)
C3-C4-C4a	119.4 (3)	N11-C11a-N12	147.1 (3)
C4-C4a-N5	129.2 (3)	C11a-N11-C6a	103.5 (3)
C4a-N5-C5a	103.2 (3)	C11a-C5a-N5	113.1 (3)
N5-C5a-N6	133.4 (2)	C11a-C5a-N6	113.4 (3)
C5a-N6-C6a	103.4 (3)	C11a-N12-C1	132.3 (3)
N6-C6a-C7	129.8 (4)	C11a-N12-C4a	103.6 (3)
C6a-C7-C8	119.6 (4)	N12-C1-O	123.1 (3)
C7-C8-N9	121.5 (4)	N12-C1-N2	113.3 (3)
C8-N9-C10	124.3 (3)	N12-C4a-C4	117.4 (3)
C8-N9-C15	117.8 (3)	N12-C4a-N5	113.4 (3)
C10-N9-C15	117.8 (3)	N12-C11a-C5a	106.7 (3)
N9-C10-N11	113.0 (3)	C1-N12-C4a	123.8 (3)
N9-C10-O10	124.0 (3)	N2-C13-C14	112.0 (3)
O10-C10-N11	122.9 (3)	N9-C15-C16	111.6 (4)

350 nm (absolute EtOH). The bond lengths and angles for **14** are given in Table IV.

The bond lengths are unexceptional when compared with the corresponding bonds in the imidazopyrimidinone portion of **7b**. The most notable difference in angles for the two syn compounds **7b** and **14** lies in the external angles to the 1,3,4,6-tetraazapentalene ring system, particularly in the bay region. The N11-C11a-N12 angle is further spread in **14** to 147.1 (3)° and the C11a-N12-C1 angle is 132.3 (3)° (see Figures 1 and 3). The spreading is also indicated in a comparison of the N5-N6 distance, 2.517 (4) Å, with the N11-N12 distance, 2.663 (4) Å, on the bay side of the tetracyclic ring system in **14**. The distance being O1 and O10 in **14** is 2.762 (3) Å, there is out-of-plane avoidance of the carbonyl oxygens, the ring structure is warped, and the ethyl groups appear on the same side of the molecule in the crystal.[2] In the crystal, there are three weak intermolecular contacts: N5···H14a, 2.64 (4) Å; O10···H3, 2.45 (4) Å; and N6···H15a, 2.67 (4) Å. The first and second of these have the geometry for hydrogen bonding: N5···H14a-C14, 3.615 (5) Å, 167 (3)°; and O10···H3-C3, 3.392 (5) Å, 168 (3)°.

The syn to anti rearrangement of **14** to **15** was effected with 0.4 M $NaOCH_3$ in methanol as in the case of **7b** to **8b**. 2,8-Diethylpyrimido[1″,6″:3′,2′]imidazo[4′,5′:4,5]imidazo[1,2-*c*]pyrimidine-1,7(2*H*,8*H*)-dione (**15**), which was obtained in 74% yield, was faster moving on silica gel TLC, R_f 0.60, than the syn isomer, R_f 0.47 (10% MeOH/$CHCl_3$). The proton NMR spectra of **14** and **15** are similar, while the longest wavelength UV absorption maximum for the anti isomer is at 362 nm (MeOH) and of greater intensity than that at 351 nm for the syn isomer. Final confirmation of the structure of the anti isomer was obtained by X-ray analysis (Table V, Figure 4). The bond lengths and angles are very close to the corresponding values for the imidazopyrimidinone portion of **8b**. The external angles to the 1,3,4,6-tetraazapentalene central system do not indicate a spreading on one side. This is as expected; the molecule is centrosymmetric, the ring system is essentially planar, and the ethyl groups are on opposite sides of the tetracyclic ring plane.[2] The N5-N6 distance is 2.592 (4) Å

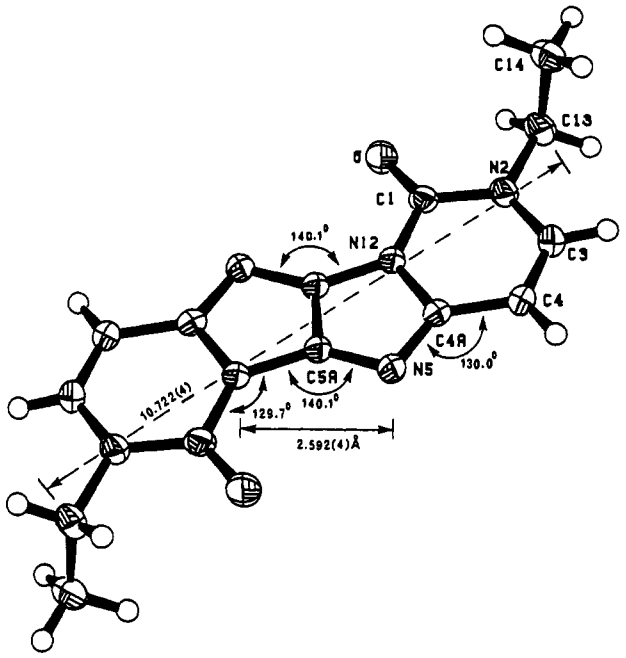

Figure 4. Single ORTEP drawing of 2,8-diethylpyrimido[1″,6″:3′,2′]-imidazo[4′,5′:4,5]imidazo[1,2-*c*]pyrimidine-1,7-dione, with the atom numbering, based on the X-ray crystal structure.

Table V. Selected Bond Lengths and Angles for **15**

bond	length, Å (esd)	bond	length, Å (esd)
O-C1	1.219 (2)	C5a-C5a	1.355 (2)
C1-N2	1.373 (2)	(C5a-C11a)	
N2-C3	1.386 (2)	C5a-N12	1.388 (2)
C3-C4	1.336 (2)	(C11a-N12)	
C4-C4a	1.421 (2)	N12-C1	1.390 (2)
C4a-N5	1.328 (2)	N12-C4a	1.415 (2)
N5-C5a	1.369 (2)	N2-C13	1.475 (2)
		C13-C14	1.507 (3)

atoms	angle, deg (esd)	atoms	angle, deg (esd)
O-C1-N2	124.7 (1)	C5a-C5a-N12	104.8 (1)
C1-N2-C3	123.1 (1)	(C5a-C11a-N12)	
C1-N2-C13	117.9 (1)	C5a-N12-C1	129.7 (1)
C3-N2-C13	118.9 (1)	(C11a-N12-C1)	
N2-C3-C4	122.9 (1)	C5a-N12-C4a	104.7 (1)
C3-C4-C4a	118.3 (1)	(C11a-N12-C4a)	
C4-C4a-N5	130.0 (1)	N12-C1-O	121.7 (1)
C4a-C4a-C5a	101.8 (1)	N12-C1-N2	113.5 (1)
N5-C5a-N6	140.1 (1)	N12-C4a-C4	116.4 (1)
(N5-C5a-N12)		N12-C4a-N5	113.6 (1)
N5-C5a-C5a	115.2 (1)	C1-N12-C4a	125.7 (1)
(N5a-C5a-C11a)		N2-C13-C14	111.8 (2)

and the C13-C15 distance is 10.722 (4) Å. The most logical reaction pathway for the conversion **14** → **15** is parallel to that envisioned for **7b** → **8b** (see above), which would function to relieve the steric strain and remove the oxygen-oxygen compression inherent in the structure **14**.

In the ribosyl-substituted series, compound **16**[8,9] was synthesized by the same route as **14**, starting with 2′,3′,5′-tri-*O*-acetylcytidine and chloroketene diethyl acetal. Under mild conditions, e.g., 0.2 M *tert*-butylamine in methanol at −5 to −10 °C for 2 h, the bulky nucleophile did not attack the pyrimidinone carbonyl, and the O-deacetylated product **17** was obtained satisfactorily with the syn ring system intact (Scheme III).[9] The C13-C15 distance, 8.065 (5) Å, determined by X-ray analysis of **14**, can be regarded as commensurate with the C1′-C1′ distance in **17**. The value is close to that derived, 8.2 Å, from the atomic coordinates for the "half"-molecule, εCyd.[9,19,20] When the hexaacetate **16** was treated

(19) Wang, A. H.-J.; Barrio, J. R.; Paul, I. C. *J. Am. Chem. Soc.* **1976**, *98*, 7401.

Scheme III

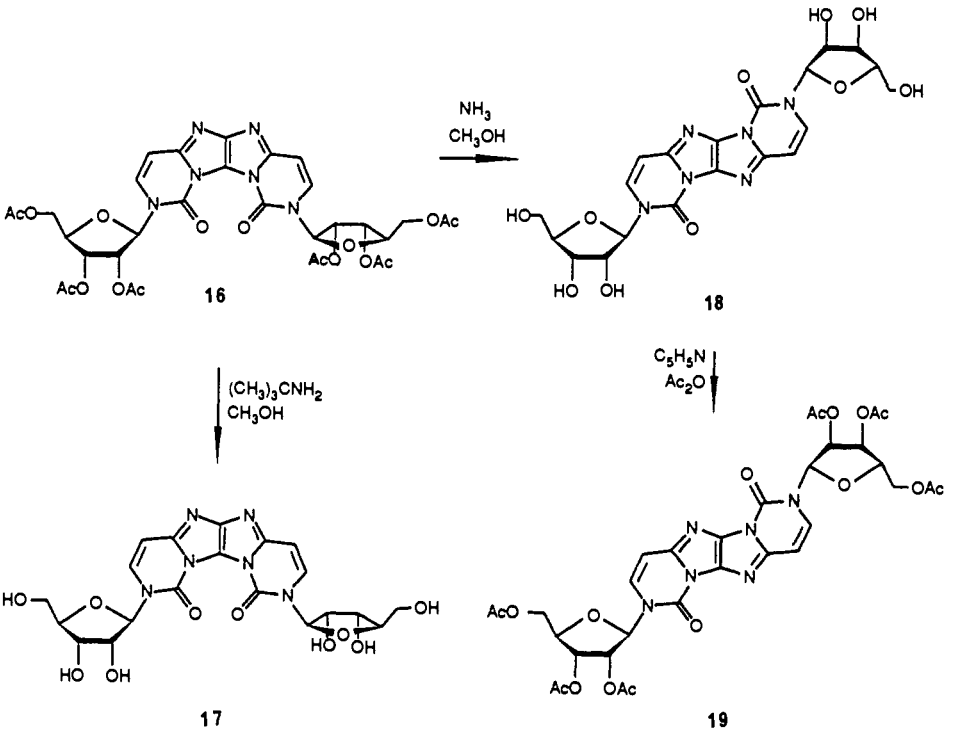

under vigorous O-deblocking conditions, namely, methanolic ammonia at 30 °C for 24 h, a single deprotected product, $C_{20}H_{22}N_6O_{10}$, was obtained in 90% yield (Scheme III). This isomer of **17** was established as anti (**18**) since the longest wavelength UV absorption maximum was at 362 nm (ϵ = 33 200), as it was also in the reacetylated derivative (**19**), i.e., 362 nm (ϵ = 36 600) (MeOH). Compound **19** was faster moving on silica gel chromatography (R_f 0.70) than **16** (R_f 0.53). The relative R_f's and UV maxima were valuable for differentiating between **14** and **15** and **16** and **19**. The ^{1}H NMR spectra of the members of these pairs, which are strikingly similar, are less valuable for this purpose. The synthetic methodology here described makes it possible to obtain syn and anti isomers in this series at will.

Compound **18**, which is a covalently linked analogue of the hydrogen-bonded construct shown in **9**, becomes especially interesting as the case unfolds for base pairing in a double-helical polynucleotide with *parallel* strands. In a theoretical helix based upon this covalent cross section, **18** is centrosymmetric and the dyad axis relating the ribosyl (also deoxyribosyl) groups in anti conformation would be perpendicular to the base-pair plane and would be coincidental with the helix axis.[21,22] The sugar phosphate backbones are 180° apart, and the C1′–C1′ distance would be expected to be close to the C13–C15 distance, 10.722 (4) Å, determined for compound **15**.[23] The structural result is that there would be only one type of groove in such a helix.

Force field calculations of Pattabiraman[24] showed that a parallel, right-handed double-helical structure with reverse (that is, N1···H–N3, N6–H···O2) Watson–Crick base pairing for poly d(A)·poly d(T)[25] is about as favorable as the normal antiparallel structure with Watson–Crick base pairing.[26] In addition, theoretical evidence was advanced by Kuryavyi[27] to show that several models of parallel DNA, and conjugation of antiparallel forms of DNA, exist. "Parallel-stranded DNA" (ps DNA or ↑↑ DNA) was then constructed in the form of two hairpins with $(dA)_{10}$·$(dT)_{10}$ stems having either two 3′-termini or two 5′-termini, and these were compared with two similar hairpins that had the normal 5′–3′ polarity (aps DNA or ↑↓ DNA).[28] Parallel orientation of strands was also achieved by introduction of a 5′–5′ phosphodiester linkage in the hairpin loop of $d(T_8)C_4(A_8)$, and the resulting structure was compared with the same sequence joined by 5′–3′ linkages.[29] A second means of imposing parallel orientation of the strands comprising a duplex was with bimolecular DNA of appropriate sequences of A and T residues such that complementarity led to parallel or, for comparison, antiparallel double helices.[30] Further comparison of ps-DNA hairpins and linear duplexes with their aps-DNA counterparts has included gel electrophoretic mobility, helix–coil transitions, spectroscopic properties, and enzyme substrate properties.[31-34]

The template cross section (**18**) that we have devised is capable of elaboration by attachment of suitable ribonucleotide bases to initiate (chemically) a parallel-stranded RNA duplex. In similar experiments, if 5-methyl-2′-deoxycytidine were to be used in place of cytidine (see Schemes II and III), the resulting template cross section would guide the attachment of deoxyribonucleotide units so as to create a parallel-stranded DNA duplex. It has been pointed out that recognition of ps-DNA by several DNA processing enzymes raises the distinct possibility that ps-DNA structures are of biological relevance.[34]

Experimental Section

Melting points were determined on a Thomas-Hoover capillary melting point apparatus and are uncorrected. ^{1}H NMR spectra were recorded on a General Electric QE-300 spectrometer at 300 MHz.

(20) Jakolski, M.; Kryzosiak, W.; Sierzputowska-Gracz, H.; Wiewiorowski, M. *Nucleic Acids Res.* **1981**, *9*, 5423.
(21) Reference 18a, p 298.
(22) The shorthand designation U⋂n can be used to represent the two fused five-membered rings as the covalent restrictor of the anti, centrosymmetric, U-like termini.
(23) Recall that the C1′–C1′ distance for a Watson–Crick A·T base pair is 10.8 Å.
(24) Pattabiraman, N. *Biopolymers* **1986**, *25*, 1603.
(25) ↑↑ Poly d(A)·poly d(T), also ↑↑ DNA, ps.
(26) ↑↓ Poly d(A)·poly d(T), also ↑↓ DNA, aps.
(27) Kuryavyi, V. V. *Mol. Biol.* **1987**, *21*, 1486.
(28) van de Sande, J. H.; Ramsing, N. B.; Germann, M. W.; Elhorst, W.; Kalisch, B. W.; v. Kitzing, E.; Pon, R. T.; Clegg, R. C.; Jovin, T. M. *Science* **1988**, *241*, 551.
(29) Germann, M. W.; Vogel, H. J.; Pon, R. T.; van de Sande, J. H. *Biochemistry* **1989**, *28*, 6220.
(30) Ramsing, N. B.; Jovin, T. M. *Nucleic Acids Res.* **1988**, *16*, 6659.
(31) Germann, M. W.; Kalisch, B. W.; van de Sande, J. H. *Biochemistry* **1988**, *27*, 8302.
(32) Ramsing, N. B.; Rippe, K.; Jovin, T. M. *Biochemistry* **1989**, *28*, 9528.
(33) Rippe, K.; Ramsing, N. B.; Jovin, T. M. *Biochemistry* **1989**, *28*, 9536.
(34) Rippe, K.; Jovin, T. M. *Biochemistry* **1989**, *28*, 9542.

Tetramethylsilane was used as an internal standard in all NMR spectra. The following abbreviations are used: s, singlet; d, doublet; t, triplet; m, multiplet; and, ex, exchangeable with D_2O. Fast-atom bombardment (FAB) mass spectra were obtained on a VG ZAB-1 HF spectrometer. Ultraviolet (UV) spectra were obtained on a Beckman Acta MVI spectrophotometer. Fluorescence excitation and emission spectra were recorded on a Spex Fluorolog 111C spectrofluorometer coupled with a Datamate microprocessor. Elemental analyses were performed by Tom McCarthy and his staff at the University of Illinois.

X-ray Crystallographic Analysis. Satisfactory samples for analysis were obtained by crystallization from methanol of **7b**, **8b**, **14**, and **15**. The reflections were observed on a Syntex $P2_1$ automated diffractometer (**7b**, **8b**, **15**) or an Enraf-Nonius CAD 4 automated *k*-axis diffractometer (**14**) equipped with a graphite monochromator using Mo Kα (λ = 0.71073 Å) radiation (Table I). The variable-scan option was used at 2–15°/min for **7b** and **8b**, 2–8°/min for **14**, and 6°/min for **15**. Three standard reflections were monitored every 100 reflections for **7b**, **8b**, and **15** and per 5400-s exposure time for **14**. There was no change in the appearance of the samples during the experiments. Anomalous dispersion and Lorentz and polarization effects[35] were applied for data correction.

The structures were solved by the direct methods program SHELXS-86.[36] Correct positions for all non-hydrogen atoms were deduced from an *E* map. Subsequent least-squares difference Fourier calculations revealed positions for the hydrogen atoms; however, for **7b** and **14**, hydrogen atoms were included as fixed contributors in "idealized" positions. In the final cycle of least-squares calculations, anisotropic thermal coefficients were refined for the non-hydrogen atoms, a group isotropic thermal parameter was varied for the hydrogen atoms, and an empirical isotropic extinction parameter was refined. Successful convergence was indicated by the maximum shift/error for the last cycle. There were no significant features in the final difference Fourier map. A final analysis of variance between observed and calculated structure factors showed no apparent systematic errors.

***N*-(8-Pyridinyl)-3-(2,3,5-tri-*O*-acetyl-β-D-ribofuranosyl)imidazo[2,1-*i*]purin-8-amine (4a).** A solution of tri-*O*-acetyladenosine (1.2 g, 3 mmol), chloroketene diethyl acetal (**11**;[37] 1.8 g, 12 mmol), and *p*-toluenesulfonic acid (0.075 g, 0.4 mmol) in dry ethyl acetate (75 mL) was stirred at room temperature for 16 h.[7,9,10] The solvent was removed under reduced pressure and the excess of chloroketene diethyl acetal was removed by codistillation with dry DMF (4 × 30 mL). The oil thus obtained was dried under high vacuum for 4 h and dissolved in a mixture of dry benzene (10 mL) and DMF (2 mL). To this were added 2-aminopyridine (0.3 g, 3.3 mmol) and *p*-toluenesulfonic acid (0.03 g, 0.17 mmol). The reaction mixture was stirred at 70 °C for 15 h. Solvent was removed in vacuo, and the residue was purified by column chromatography on silica gel using as eluent a gradient of 5–50% MeOH/CH_2Cl_2 (v/v). Appropriate fractions were combined and concentrated to give a solid that was further purified by radial preparative-layer chromatography on a Chromatotron instrument using silica gel, eluent 5% MeOH/$CHCl_3$ (v/v). The product thus obtained was recrystallized from acetone to give **4a** as a colorless solid: yield, 0.650 g (45%); mp 194 °C; ^{1}H NMR ($(CD_3)_2SO$) δ 9.99 (s, 1, NH, ex), 9.30 (s, 1, 2-H), 8.51 (s, 1, 5-H), 8.34 (s, 1, 7-H), 8.27 (d, J = 4.5 Hz, 1, 6″-H), 7.60 (m, 1, 4″-H), 7.03 (d, J = 8.4 Hz, 1, 3″-H), 6.79 (m, 1, 5″-H), 6.34 (d, J = 5.4 Hz, 1, 1′-H), 6.06 (t, J = 5.7 Hz, 1, 2′-H), 5.66 (t, J = 5.1 Hz, 1, 3′-H), 4.41 (m, 2, 4′-H, 5′a-H), 4.28 (m, 1, 5′b-H), 2.14, 2.05, and 2.04 (3 s, 9, $COCH_3$); UV, λ_{max} (MeOH) 297, 264 nm; low-resolution FAB mass spectrum, m/z 510 (MH^+), 252 (B^+ + 2); high-resolution FAB mass spectrum, m/z 510.1742 ($C_{23}H_{24}N_7O_7$ requires 510.1737 amu).

***N*-(2-Pyridinyl)-5,6-dihydro-5-oxo-6-(2,3,5-tri-*O*-acetyl-β-D-ribofuranosyl)imidazo[1,2-*c*]pyrimidin-2-amine (5a).** A solution of 2′,3′,5′-tri-*O*-acetylcytidine (4 g, 10.8 mmol) and chloroketene diethyl acetal (**11**;[37] 4 g, 26.6 mmol) in dry CH_3CN was stirred at room temperature for 24 h. Solvent was removed under vacuum and excess of chloroketene diethyl acetal was removed by codistillation with dry DMF (5 × 15 mL).[8-10] The residue was dried under high vacuum for an additional 5 h, dissolved in dry DMF (50 mL), and heated with 2-aminopyridine (1.22 g, 12.97 mmol) at 60–65 °C for 24 h. The reaction mixture was concentrated to an oily residue, which was purified by flash chromatography on silica gel using 7% MeOH/$CHCl_3$ (v/v) as the eluent. Removal of the solvent gave **5a** as a foam, which was recrystallized from ethanol as a colorless solid: yield 1.1 g (21%); mp 166–167 °C; ^{1}H NMR ($(CD_3)_2SO$) δ 9.80 (s, 1, NH, ex), 8.26 (d, J = 4.5 Hz, 1, 6″-H), 7.96 (s, 1, 3-H), 7.56 (m, 2, 7-H, 4″-H), 6.98 (d, J = 8.4 Hz, 1, 3″-H), 6.77 (m, 1, 5′-H), 6.72 (d, J = 7.8 Hz, 1, 8-H), 6.20 (d, J = 5.1 Hz, 1, 1′-H), 5.56 (t, J = 5.4 Hz, 1, 2′-H), 5.42 (t, J = 5.4 Hz, 1, 3′-H), 4.31 (m, 3, 4′-H, 5′-H's), 2.11, 2.07, and 2.06 (3 s, 9, $COCH_3$); UV, λ_{max} (MeOH) 315, 259, 254 nm; low-resolution FAB mass spectrum, m/z 486 (MH^+), 228 (B^+ + 2). Anal. Calcd for $C_{22}H_{23}N_5O_8$: C, 54.43; H, 4.74; N, 14.43. Found: C, 54.57; H, 4.73; N, 14.45.

***N*-(2-Pyridinyl)-5,6-dihydro-6-ethyl-5-oxoimidazo[1,2-*c*]pyrimidin-2-amine (5b).** Compound **5b** was prepared from 1-ethylcytosine[12] (0.5 g, 4 mmol) and 2-aminopyridine (0.8 g, 8.5 mmol) by a procedure similar to that described for the preparation of **5a**: yield 0.275 g (30%); mp 215–216 °C; ^{1}H NMR ($(CD_3)_2SO$) δ 9.73 (s, 1, NH, ex), 8.26 (d, J = 4.5 Hz, 1, 6′-H), 7.96 (s, 1, 3-H), 7.53 (m, 2, 7-H, 4′-H), 6.99 (d, J = 8.7 Hz, 1, 3′-H), 6.76 (m, 1, 5′-H), 6.57 (d, J = 7.8 Hz, 1, 8-H), 3.98 (q, J = 7.2 Hz, 2, CH_2), 1.30 (t, J = 7.2 Hz, 3, CH_3); UV, λ_{max} (MeOH) 316, 260, and 254 nm; low-resolution FAB mass spectrum, m/z 256 (MH^+). Anal. Calcd for $C_{13}H_{13}N_5O$: C, 61.17; H, 5.13; N, 27.43. Found: C, 61.22; H, 5.16; N, 27.67.

3-(2,3,5-Tri-*O*-acetyl-β-D-ribofuranosyl)-3*H*-pyrido[1″,2″:1′,2′]-imidazo[2,1-*i*]purine (6a). A solution of iodobenzene diacetate (0.2 g, 0.62 mmol) in trifluoroethanol (10 mL) was added slowly to a stirred solution of **4a** (0.2 g, 0.39 mmol) in trifluoroethanol (15 mL). After the addition was complete (15 min), the reaction mixture was stirred for an additional 30 min. Solvent was removed in vacuo, and the residue was purified by flash chromatography on silica gel, 5–10% MeOH/$CHCl_3$ (v/v) as eluent. Appropriate fractions were combined and concentrated to furnish a light yellow solid which, after crystallization from ethanol, gave colorless **6a**: yield 0.11 g (55%); mp 227–228 °C; ^{1}H NMR ($(CD_3)_2SO$) δ 9.93 (s, 1, 5-H), 9.28 (d, J = 6.9 Hz, 1, 8-H), 8.63 (s, 1, 2-H), 7.79 (d, J = 9.0 Hz, 1, 11-H), 7.45 (m, 1, 10-H), 7.17 (m, 1, 9-H), 6.43 (d, J = 5.1 Hz, 1, 1′-H), 6.10 (t, J = 5.4 Hz, 1, 2′-H), 5.69 (t, 5.4 Hz, 1, 3′-H), 4.47 (m, 2, 4′-H, 5′a-H), 4.3 (m, 1, 5′b-H), 2.15, 2.07, and 2.05 (3 s, 9, $COCH_3$); UV λ_{max} (MeOH) 350 (ϵ 11 100), 334 (12 800), 300 sh (11 100), 269 (42 600), 238 (15 500), 224 nm (16 600); fluorescence λ_{max}^{em} 420 nm, λ_{max}^{ex} 350 nm, Φ = 0.15 (absolute ethanol) (relative to coumarin in absolute ethanol, Φ = 0.51 at λ^{ex} 350 nm (measured relative to the reported value of Φ = 0.64 at λ^{ex} 366 nm[5])); low-resolution FAB mass spectrum, m/z 508 (MH^+), 250 (B^+ + 2); high-resolution FAB mass spectrum, m/z 508.1591 ($C_{23}H_{22}N_7O_7$ requires 508.1580 amu).

3-(β-D-Ribofuranosyl)-3*H*-pyrido[1″,2″:1′,2′]imidazo[4′,5′:4,5]-imidazo[2,1-*i*]purine (6c). A solution of **6a** (0.05 g, 0.10 mmol) in 15 mL of anhydrous methanol saturated with ammonia was stirred at room temperature for 24 h in a sealed vessel. The mixture was concentrated in vacuo. Addition of methanol gave a solid, which was filtered and washed with methanol (5 mL) to give colorless **6c**: yield 0.028 g (74%); mp 270–271 °C; ^{1}H NMR ($(CD_3)_2SO$) δ 9.89 (s, 1, 5-H), 9.26 (d, J = 6.6 Hz, 1, 8-H), 8.67 (s, 1, 2-H), 7.79 (d, J = 9.3 Hz, 1, 11-H), 7.44 (m, 1, 10-H), 7.17 (m, 1, 9-H), 6.12 (d, J = 5.4 Hz, 1, 1′-H), 5.60 (d, J = 6 Hz, 1, OH, ex), 5.31 (d, J = 5.1 Hz, 1, OH, ex), 5.14 (t, J = 5.4 Hz, 1, OH, ex), 4.64 (m, 1, 2′-H), 4.21 (m, 1, 3′-H), 4.01 (m, 1, 4′-H), 3.71 (m, 1, 5′a-H), 3.62 (m, 1, 5′b-H); UV, λ_{max} (MeOH) 350, 337, 301 (sh), 270, 238, 230 nm; low-resolution FAB mass spectrum, m/z 382 (MH^+), 250 (B^+ + 2); high-resolution FAB mass spectrum, 382.1263 ($C_{17}H_{16}N_7O_4$ requires 382.1263).

2-(2,3,5-Tri-*O*-acetyl-β-D-ribofuranosyl)pyrido[1″,2″:1′,2′]imidazo-[4′,5′:4,5]imidazo[1,2-*c*]pyrimidin-1-one (7a). This compound was prepared by treating **5a** (0.19 g, 0.39 mmol) with iodobenzene diacetate (0.135 g, 0.41 mmol) in trifluoroethanol at room temperature for 30 min as reported for the preparation of **6a**: yield 0.095 g (50%); mp 140–143 °C; ^{1}H NMR ($(CD_3)_2SO$) δ 9.09 (d, J = 6.6 Hz, 1, 10-H), 7.70 (m, 2, 3-H, 7-H), 7.36 (m, 1, 8-H), 7.08 (m, 1, 9-H), 6.95 (d, J = 7.8 Hz, 1, 4-H), 6.27 (d, J = 4.8 Hz, 1, 1′-H), 5.65 (t, 4.8 Hz, 1, 2′-H), 5.45 (t, J = 5.1 Hz, 1, 3′-H), 4.37 (m, 3, 4′-H, 5′-H's), 2.11, 2.09, and 2.07 (3 s, 9, $COCH_3$); UV λ_{max} (MeOH) 364 (ϵ 10 000), 346 (13 900), 334 (sh) (11 800), 323 (sh) (9900), 265 (17 000), 228 nm (28 600); fluorescence, λ_{max}^{em} 395, 416 (sh) nm, λ_{max}^{ex} 350 nm, Φ = 0.28 (absolute ethanol) (relative to coumarin in absolute ethanol Φ = 0.51 at λ^{ex} = 350 nm (measured relative to reported value of Φ = 0.64 at λ^{ex} 366 nm)); low-resolution FAB mass spectrum, m/z 484 (MH^+), 226 (B^+ + 2); high-resolution FAB mass spectrum, 484.1464 ($C_{22}H_{22}H_5O_8$ requires 484.1468 amu). Anal. Calcd for $C_{22}H_{21}N_5O_8 \cdot {}^1/_2H_2O$: C, 53.66; H, 4.50; N, 14.22. Found: C, 53.75; H, 4.25; N, 14.18.

2-Ethylpyrido[1″,2″:1′,2′]imidazo[4′,5′:4,5]imidazo[1,2-*c*]pyrimidin-1-one (7b). An experimental procedure similar to that described for the preparation of **6b** was employed to prepare **7b** from **5b** (0.395 g, 1.54 mmol) and iodobenzene diacetate (0.350 g, 1.08 mmol): yield 0.225 g (58%); mp 261–262 °C; ^{1}H NMR ($(CD_3)_2SO$) δ 9.12 (d, J = 6.6 Hz, 1, 10-H), 7.65 (m, 2, 7-H, 3-H), 7.33 (m, 1, 8-H), 7.03 (m, 1, 9-H), 6.78 (d, J = 7.5 Hz, 1, 4-H), 4.05 (q, J = 7.2 Hz, 2, CH_2), 1.34 (t, J = 7.2

(35) Stout, G. H.; Jensen, L. H. *X-ray Structure Determination, A Practical Guide*; MacMillan: New York, 1968; pp 195–200, 234–237.

(36) Sheldrick, G. M. *SHELXS-86, Crystallographic Computing 3*; Sheldrick, G. M., Kruger, C., Goddard, R., Eds.; Oxford University Press: Oxford, 1985; pp 175–189.

(37) *Caution! Chloroketene diethyl acetal is a mutagen and should be handled with caution in a well-ventilated hood, with suitable trapping.*

Hz, 3, CH_3); UV λ_{max} (H_2O, pH 7) 361 (ε 13 400), 344 (17 200), 333 (sh) (14 400), 267 (16 000), 230 nm (38 400); λ_{max} (H_2O, pH 1) 351 (ε 16 200), 337 (19 800), 309 (sh) (10 100), 296 (sh) (6500), 255 (12 200), 222 nm (38 800); λ_{max} (H_2O, pH 11) 361 (ε 12 100), 344 (16 200), 330 (sh) (13 000), 268 (15 000), 230 nm (35 200); fluorescence, λ_{max}^{em} nm 393, 412 (sh) nm, λ_{max}^{ex} 350 nm, Φ = 0.32 (absolute ethanol); low-resolution FAB mass spectrum, *m/z* 254 (MH^+). Anal. Calcd for $C_{13}H_{11}N_5O$: C, 61.66; H, 4.34; N, 27.66. Found: C, 61.31; H, 4.33; N, 27.64.

2-(β-D-Ribofuranosyl)pyrido[1″,2″:1′,2′]imidazo[4′,5′:4,5]imidazo[1,2-*c*]pyrimidin-1-one (7c). A solution of **7a** (0.120 g, 0.248 mmol) in 0.2 M *tert*-butylamine in methanol (15 mL) was stirred at −5 to −10 °C for 2 h. The solid that separated was collected by filtration, washed with dry CH_2Cl_2 (10 mL) and absolute ethanol (3 × 10 mL), and dried under high vacuum to give colorless solid: yield 0.070 g (79%); mp 248–250 °C; ^1H NMR ($(CD_3)_2SO$) δ 9.13 (d, *J* = 6.9 Hz, 1, 10-H), 7.94 (d, *J* = 8.1 Hz, 1, 3-H), 7.68 (d, *J* = 9 Hz, 1, 7-H), 7.36 (m, 1, 8-H), 7.07 (m, 1, 9-H), 6.86 (d, *J* = 8.1 Hz, 1, 4-H), 6.13 (d, *J* = 4.8 Hz, 1, 1′-H), 5.53 (d, *J* = 5.4 Hz, 1, OH, ex), 5.23 (m, 2, OH), 4.21 (m, 1, 2′-H), 4.08 (m, 1, 3′-H), 3.98 (m, 1, 4′-H), 3.71 (m, 2, 5′-CH_2); UV λ_{max} (MeOH) 364 (ε 11 800), 347 (15 700), 336 (sh) (12 900), 269 (16 300), 230 nm (34 400); fluorescence, λ_{max}^{em} 393, 417 (sh) nm, λ_{max}^{ex} 350 nm, Φ = 0.32 (absolute ethanol); low-resolution FAB mass spectrum, *m/z* 358 (MH^+), 226 (B^+ + 2); high-resolution FAB mass spectrum, 358.1149 ($C_{16}H_{16}N_5O_5$ requires 358.1151 amu).

2-Ethylpyrido[2″,1″:2′,3′]imidazo[4′,5′:4,5]imidazo[1,2-*c*]pyrimidin-1-one (8b). A solution of **7b** (0.045 g, 0.177 mmol) in 0.4 M $NaOCH_3$ in MeOH (10 mL) was refluxed for 5 h. Aqueous acetic acid (10% v/v, 0.5 mL) was added to the reaction mixture, solvent was removed under reduced pressure, and the residue was purified by column chromatography using MeOH/$CHCl_3$ (3% v/v) as the eluent. Appropriate fractions were combined and concentrated to give a light yellow solid which, after recrystallization from methanol, furnished light yellow crystalline **8b**: yield 0.030 g (67%); mp 279–280 °C; ^1H NMR ($(CD_3)_2SO$) δ 8.71 (d, *J* = 6.6 Hz, 1, 7-H), 7.75 (d, *J* = 9.3 Hz, 10-H), 7.62 (d, *J* = 7.8 Hz, 3-H), 7.37 (m, 1, 9-H), 7.07 (m, 1, 8-H), 6.76 (d, *J* = 7.8 Hz, 1, 4-H), 4.02 (q, *J* = 7.2 Hz, 2, CH_2), 1.32 (t, *J* = 7.2 Hz, 3, CH_3); UV, λ_{max} (H_2O, pH 7) 372 (ε 17 600), 353 (24 500), 340 (sh) (21 000), 274 (8900), 261 (9700), 241 (18 800), 229 nm (25 100); λ_{max} (H_2O, pH 1) 340 (ε 23 700), 280 (5700), 237 nm (21 900); λ_{max} (H_2O, pH 11) 372 (ε 15 800), 353 (20 400), 336 (sh) (18 600), 274 (7300), 261 (7700), 241 (15 200), 230 nm (28 300); fluorescence, λ_{max}^{em} 419 nm, λ_{max}^{ex} 350 nm, Φ = 0.70 (absolute ethanol); low-resolution FAB mass spectrum, *m/z* 254 (MH^+). Anal. Calcd for $C_{13}H_{11}N_5O \cdot {}^1/_4H_2O$: C, 60.58; H, 4.50; N, 27.17. Found: C, 60.67; H, 4.33; N, 27.16.

2-(β-D-Ribofuranosyl)pyrido[2″,1″:2′,3′]imidazo[4′,5′:4,5]imidazo[1,2-*c*]pyrimidin-1-one (8c). A solution of **7a** (0.10 g, 0.206 mmol) in anhydrous methanol saturated with ammonia (25 mL) was stirred at room temperature for 60 h in a sealed vessel. After removal of the solvent in vacuo, addition of methanol gave a solid, which was filtered and dried. Recrystallization from aqueous ethanol (30:70) gave **8c** as a colorless solid: yield 0.066 g (89%); mp 300 °C; ^1H NMR ($(CD_3)_2SO$) δ 8.72 (d, *J* = 6.3 Hz, 1, 7-H), 7.86 (d, *J* = 8.1 Hz, 1, 3-H), 7.76 (d, *J* = 9.6 Hz, 1, 10-H), 7.39 (m, 1, 9-H), 7.11 (m, 1, 8-H), 6.83 (d, *J* = 8.1 Hz, 1, 4-H), 6.14 (d, *J* = 5.4 Hz, 1, 1′-H), 5.51 (d, *J* = 5.4 Hz, 1, OH, ex), 5.20 (m, 2, OH), 4.19 (m, 1, 2′-H), 4.06 (m, 1, 3′-H), 3.96 (m, 1, 4′-H), 3.64 (m, 2, 5′-H's); UV, λ_{max} (MeOH) 374 (ε 14 300), 355 (20 700), 338 (sh) (17 900), 262 (8600), 232 (22 200); fluorescence, λ_{max}^{em} 419 nm, λ_{max}^{ex} 350 nm, Φ = 0.74 (absolute ethanol); high-resolution FAB mass spectrum, *m/z* 358.1146 ($C_{16}H_{16}N_5O_5$ requires 358.1151 amu). Anal. Calcd for $C_{15}H_{15}N_5O_5$: C, 53.78; H, 4.23; N, 19.60. Found: C, 53.58; H, 4.30; N, 19.40.

2-(2,3,5-Tri-*O*-acetyl-β-D-ribofuranosyl)pyrido[2″,1″:2′,3′]imidazo[4′,5′:4,5]imidazo[1,2-*c*]pyrimidin-1-one (8a). A solution of **8c** (0.050 g, 0.140 mmol) in anhydrous pyridine (0.5 mL) and acetic anhydride (0.3 mL) was stirred at room temperature for 12 h. After removal of the solvent in vacuo, the residue was purified by column chromatography using 5% MeOH/$CHCl_3$ as the eluent. The appropriate fractions were concentrated and the solid obtained was crystallized from $CHCl_3$/pentane (10:90 v/v) to give **8a**: yield 0.060 g (89%); mp 164–166 °C; ^1H NMR ($(CD_3)_2SO$) δ 8.75 (d, *J* = 6.6 Hz, 1, 7-H), 7.76 (d, *J* = 9.6 Hz, 1, 10-H), 7.64 (d, *J* = 8.1 Hz, 1, 3-H), 7.39 (m, 1, 9-H), 7.10 (m, 1, 8-H), 6.91 (d, *J* = 8.1 Hz, 1, 4-H), 6.25 (d, *J* = 4.8 Hz, 1, 1′-H), 5.62 (t, *J* = 4.8 Hz, 1, 2′-H), 5.45 (t, *J* = 5.1 Hz, 1, 3′-H), 4.38 (m, 3, 4′-H, 5′-H's), 2.12, 2.08, and 2.07 (3 s, 9, $COCH_3$); UV, λ_{max} (H_2O, pH 7) 370 (ε 23 200), 351 (32 500), 335 (sh) (27 100), 278 (sh) (10 100), 260 (11 600), 230 nm (32 900); λ_{max} (H_2O, pH 1) 350 (ε 20 900), 335 (27 100), 250 (9300), 234 nm (21 300); λ_{max} (H_2O, pH 11) 370 (ε 21 700), 352 (31 000), 338 (26 000), 276 (9700), 261 (11 200), 231 nm (29 800); fluorescence, λ_{max}^{em} nm 417, λ_{max}^{ex} 350 nm, Φ = 0.42 (absolute ethanol); low-resolution FAB mass spectrum, *m/z* 484 (MH^+), 226 (B^+ + 2); high-resolution FAB mass spectrum, 484.1464 ($C_{22}H_{22}N_5O_8$ requires 484.1468 amu). Anal. Calcd for $C_{22}H_{21}N_5O_8 \cdot {}^1/_2H_2O$: C, 53.66; H, 4.50; N, 14.22. Found: C, 53.88; H, 4.28; N, 14.03.

***N*-[4-(1,2-Dihydro-1-ethyl-2-oxopyrimidinyl)]-5,6-dihydro-6-ethyl-5-oxoimidazo[1,2-*c*]pyrimidin-2-amine (12).** A mixture of 1-ethylcytosine (**10**; 0.50 g, 3.6 mmol)[12] and chloroketene diethyl acetal (**11**;[37] 0.27 g, 1.8 mmol) in anhydrous DMF (2 mL) and benzene (2 mL) was stirred at 90 °C for 24 h under nitrogen. Solvent was removed under reduced pressure and the product mixture was purified by radial chromatography[38] on silica gel, 5–10% MeOH/$CHCl_3$ eluent, followed by recrystallization from ethanol to give **12** as tan crystals: yield 108 mg (20%); mp 240 °C; ^1H NMR ($(CD_3)_2SO$) δ 10.39 (s, 1, NH, ex), 8.07 (s, 1, 3-H), 7.78 (d, 1, *J* = 6.9 Hz), 7.55 (d, 1, *J* = 7.2 Hz), 6.60 (d, 1, *J* = 7.5 Hz), 6.05 (d, 1, *J* = 6.6 Hz), 3.98 (q, 2), 3.75 (q, 2), 1.86 (t, 3), 1.25 (t, 3); UV, λ_{max} (MeOH) 312, 240 nm; low-resolution FAB mass spectrum, *m/z* 301 (MH^+). Anal. Calcd for $C_{14}H_{16}N_6O_2$: C, 55.99; H, 5.37; N, 27.99. Found: C, 55.73; H, 5.36; N, 27.67.

2,9-Diethylpyrimido[1″,6″:1′,2′]imidazo[4′,5′:4,5]imidazo[1,2-*c*]pyrimidine-1,10(2*H*,9*H*)-dione (14). To a cold solution (−10 °C) of **12** (57 mg, 0.19 mmol) in a solvent mixture of 1,1,1,3,3,3-hexafluoro-2-methyl-2-propanol and nitromethane (1:2 v/v, 8 mL) was added 2-nitroiodobenzene diacetate (**13**, 2-nitro(diacetoxyiodo)benzene) (55 mg, 0.145 mmol)[7-9] in the same solvent (2 mL) over a period of 30 min. The reaction mixture was stirred at −10 °C for 1.5 h. Additional oxidant (**13**; 15 mg, 0.013 mmol) was added and stirring was continued at −5 °C for 30 min, at which time the starting material had been consumed according to TLC on silica gel ($CHCl_3$/MeOH, 9:1). The solvent was removed under reduced pressure, and the product was purified by flash chromatography, 5% MeOH in $CHCl_3$ as eluent, and recrystallization from methanol as colorless needles: yield 30 mg (54%); mp 281–282 °C; ^1H NMR ($(CD_3)_2SO$) δ 7.59 (d, 2, *J* = 7.8 Hz, 3-H, 8-H), 6.68 (d, 2, *J* = 7.8 Hz, 4-H, 7-H), 3.99 (q, 4, *J* = 6.9 Hz, CH_2), 1.29 (t, 6, *J* = 6.9 Hz, CH_3); UV, λ_{max} (MeOH) 351 (ε 13 400), 335 (18 000), 256 (21 500), 221 nm (25 500); fluorescence, λ_{max}^{em} 389, 410 (sh) nm; λ_{max}^{ex} 350 nm, Φ = 0.14 (absolute ethanol); low-resolution FAB mass spectrum, *m/z* 299 (MH^+). Anal. Calcd for $C_{14}H_{14}N_6O_2$: C, 56.37; H, 4.73; N, 28.18. Found: C, 56.41; H, 4.66; N, 28.19.

2,8-Diethylpyrimido[1″,6″:3′,2′]imidazo[4′,5′:4,5]imidazo[1,2-*c*]pyrimidine-1,7(2*H*,8*H*)-dione (15). This anti compound was prepared from **14** by a procedure similar to that described for **7b** → **8b** using MeO-Na/MeOH: yield 74%; mp >300 °C; ^1H NMR ($(CD_3)_2SO$) δ 7.59 (d, 2, *J* = 8.1 Hz, 3-H, 9-H), 6.77 (d, 2, *J* = 7.8 Hz, 4-H, 10-H), 4.01 (q, 4, *J* = 7.2 Hz, CH_2), 1.31 (t, 6, *J* = 7.2 Hz, CH_3); UV, λ_{max} (MeOH) 362 (ε 32 500), 343 (36 600), 326 nm (25 100); fluorescence, λ_{max}^{em} 386.5, 408.5 (sh) nm, λ_{max}^{ex} 350 nm, Φ = 0.06 (absolute ethanol); low-resolution FAB mass spectrum, *m/z* 299 (MH^+). Anal. Calcd for $C_{14}H_{14}N_6O_2$: C, 56.37; H, 4.73; N, 28.18. Found: C, 56.36; H, 4.76; N, 28.14.

2,9-Bis(2′,3′,5′-tri-*O*-acetyl-β-D-ribofuranosyl)pyrimido[1″,6″:1,2]imidazo[4′,5′:4,5]imidazo[1,2-*c*]pyrimidine-1,10(2*H*,9*H*)-dione (16) was made as described previously[8,9] and was deacetylated with *tert*-butylamine in methanol[2,9] to **2,9-bis(β-D-ribofuranosyl)pyrimido[1″,6″:1,2]imidazo[4′,5′:4,5]imidazo[1,2-*c*]pyrimidine-1,10(2*H*,9*H*)dione (17).**

2,8-Bis(β-D-ribofuranosyl)pyrimido[1″,6″:3′,2′]imidazo[4′,5′:4,5]imidazo[1,2-*c*]pyrimidine-1,7(2*H*,8*H*)-dione (18). This anti compound was obtained from **16** by a procedure similar to that used for **7a** → **8c**, using anhydrous MeOH saturated with ammonia at 30 °C for 24 h. Recrystallization from ethanol gave a light yellow solid: yield 90%; mp 242–243 °C; ^1H NMR ($(CD_3)_2SO$) δ 7.85 (d, 2, *J* = 7.8 Hz, 3-H, 9-H), 6.85 (d, 2, *J* = 7.8 Hz, 4-H, 10-H), 6.12 (d, 2, *J* = 5.1 Hz, 1′-H), 5.51 (d, 2, *J* = 5.4 Hz, ex, OH), 5.22 (m, 4, ex, OH), 4.19 (m, 2, 2′-H), 4.06 (m, 2, 3′-H), 3.95 (m, 2, 4′-H), 3.66 (m, 4, 5′-H); UV, λ_{max} (MeOH) 362 (ε 33 200), 343 (38 900), 327 nm (27 500); fluorescence, λ_{max} 384.5, 406.5 (sh) nm; λ_{max} 350 nm, Φ = 0.04 (absolute ethanol); low-resolution FAB mass spectrum, *m/z* 507 (MH^+); high-resolution FAB mass spectrum, 507.1430 ($C_{20}H_{23}N_6O_{10}$ requires 507.1475 amu).

2,8-Bis[β-D-(2′,3′,5′-tri-*O*-acetyl)ribofuranosyl]pyrimido[1″,6″:3′,2′]imidazo[4′,5′:4,5]imidazo[1,2-*c*]pyrimidine-1,7(2*H*,8*H*)-dione (19) was prepared from **18** by using pyridine and acetic anhydride according to the directions for **8c** → **8a** and was purified by silica gel chromatography, 2–3% MeOH in $CHCl_3$ as eluent. After removal of the solvent, **19** was obtained as a white fluffy solid: yield 95%; mp 190–192 °C; ^1H NMR ($(CD_3)_2SO$) δ 7.64 (d, 2, *J* = 8.1 Hz, 3-H, 9-H), 6.92 (d, 2, *J* = 8.1 Hz, 4-H, 10-H), 6.23 (d, 2, *J* = 4.8 Hz, 1′-H), 5.61 (t, 2, *J* = 5.4 Hz, 2′-H), 5.44 (t, 2, *J* = 5.1 Hz, 3′-H), 4.36 (m, 3, 4-H, 5-H), 2.06, 2.07, 2.08 (3 s, 18, $COCH_3$); UV, λ_{max} (MeOH) 362 (ε 36 600), 342 (42 700), 326 nm (31 800), fluorescence, λ_{max}^{em} 384.5, 405 (sh) nm, λ_{max}^{ex} 350 nm, Φ = 0.37 (absolute ethanol); low-resolution FAB mass spectrum, *m/z* 758

(38) By Chromatotron: Harrison Research, Inc., Palo Alto, CA.

(M^+), 759 (MH^+); high-resolution FAB mass spectrum, 758.2043 ($C_{32}H_{34}N_6O_{16}$ requires 758.2031 amu).

Acknowledgment. This work was supported by research Grant CHE 84-16336 from the National Science Foundation and by an unrestricted grant from Eli Lilly and Co. NMR data were obtained on a QE-300 spectrometer supported by NIH Grant PHS 1532135. Mass spectra were obtained on a VG ZAB-1 HF spectrometer supported by NIH Grant GM 27079. We thank Dr. Viswanathan Sasisekharan, Fogarty Scholar-in-Residence, 1989-1990, National Institutes of Health, for valuable discussion.

Registry No. 4a, 120172-85-2; **5a**, 120172-86-3; **5b**, 120172-91-0; **6a**, 120172-87-4; **6c**, 120172-89-6; **7a**, 120172-88-5; **7b**, 120172-90-9; **7c**, 120204-15-1; **8a**, 131154-63-7; **8b**, 120172-94-3; **8c**, 120172-93-2; **10**, 25855-37-2; **11**, 42520-09-2; **12**, 120172-82-9; **13**, 69180-46-7; **14**, 120204-13-9; **15**, 120204-14-0; **16**, 106160-98-9; **17**, 106139-36-0; **18**, 120172-83-0; **19**, 120172-84-1; tri-*O*-acetyladenosine, 7387-57-7; 2',3',5'-tri-*O*-acetylcytidine, 56787-28-1; 2-aminopyridine, 504-29-0.

Supplementary Material Available: Final atomic positional parameters, anisotropic thermal properties, torsion angles, bond lengths and angles, and graphics from X-ray structure determinations of **7b**, **8b**, **14**, and **15** (121 pages); observed and calculated structure factors (21 pages). Ordering information is given on any current masthead page.

Amide Chemical Shifts in Many Helices in Peptides and Proteins Are Periodic

I. D. Kuntz,* P. A. Kosen, and E. C. Craig

Contribution from the Department of Pharmaceutical Chemistry, University of California, San Francisco, California 94143-0446. *Received August 16, 1990*

Abstract: A survey of the literature data on the NMR chemical shifts of amide hydrogens in peptides and proteins finds many cases in which resonances in helical structures show a periodicity of ca. 3-4 residues/cycle. Some helices do not show such behavior, nor do α carbon hydrogen resonances. The simplest explanation is that the helical curvature found by high-resolution X-ray crystallographic studies for some helices in proteins is a fairly general phenomenon for protein and peptide structures in solution.

Introduction

There have been several reports[1-5] that the mean chemical shift of amide protons is approximately 0.2 ppm upfield in helical structures and approximately 0.3 ppm downfield in β sheet structures. We add the further observation that, in many cases, the helical component is periodic in character, with a dominant repeat near 3.6 residues. The most striking example is a coil-coil peptide: the leucine zipper[6] (Figure 1). The periodicity is obvious for residues 10-31 of the leucine zipper, and, on analysis, accounts for 65% of the sequential variation in chemical shift for these amide protons. Other examples abound in proteins and peptides (Table I; see also ref 5, Figure 1).

Methods and Results

We used three methods to extract the periodic contribution to the chemical shifts. Simple plots of chemical shift vs sequence[5] allow a visual assessment. For such plots, we used the criterion that the spacing of three maximum of three minima corresponded to periodicity of α helices (i; $i + 3$ or $i + 4$; $i + 7$). For sequences that met this standard, we estimated the peak-to-peak value of the sinusoidal component (Table I). The second method used a linear prediction method to calculate the dominant periodicity over an arbitrary window[7] (Table I). Finally, Fourier coefficients can be extracted by using the formula given by Eisenberg et al.[8] In Table I we give the average amplitude (ca. 40% of the peak-to-peak value for sinusoids) and the fraction of the total oscillatory signal that occurs with a period of 3.6 residues/cycle.

On the basis of the data in Table I, we draw the following observations: (1) significant oscillations of the amide proton chemical shift are seen for three-fourths of the helices assigned in the data set; (2) the average helical variation is approximately 0.4 ppm in amplitude, with the maximal variations approaching 1 ppm; (3) in most cases, the downfield protons are associated with hydrophobic side chains; (4) the chemical shifts of α carbon protons do not show much periodicity, although a weak out-of-phase component (<20%) cannot be ruled out; (5) a similar oscillation with a repeat of ca. 2 residues in β sheet regions is occasionally seen (see Figure 1 in Williamson[5]) but is not a general phenomenon; (6) the dominant effect is transverse to the helical axis—there is little periodic chemical shift displacement associated with the ends of helices. Occasional nonhelical features (e.g., reverse turns) can contribute to some helix-like signal but the magnitudes are usually small.

We can also show that the amplitude of the helical variation, calculated as either the average amplitude or the maximum amplitude at 3.6 residues/cycle, is roughly proportional to the circular dichroism signal at $[\Theta]_{222}$ (Figure 2) for a small peptide in water or water/TFE solutions.

Finally, we have made a cursory inspection of ^{15}N amide and ^{13}C carbonyl assignments. Helical variations of ca. 4 ppm in the ^{15}N chemical shifts are observed for three of four helices in thioredoxin;[9] variations of ca. 4 ppm are noted for the ^{13}C carbonyl

(1) Dalgarno, D. C.; Levine, B. A.; Williams, R. J. P. *Biosci. Rep.* **1983**, *3*, 443-452.
(2) Szilágyi, L.; Jardetzky, O. *J. Magn. Reson.* **1989**, *83*, 441-449.
(3) Zuiderweg, E. R. P.; Nettesheim, N. G.; Mollison, K. W.; Carter, G. W. *Biochemistry* **1989**, *28*, 172-185.
(4) Guiles, R. D.; Altman, J.; Lipka, J.; Kuntz, I. D.; Waskell, L. *Biochemistry* **1990**, *29*, 1276-1289.
(5) Williamson, M. P. *Biopolymers* **1990**, *29*, 1423-1431.
(6) Oas, T. G.; McIntosh, L. P.; O'Shea, E. K.; Dahlquist, F. W.; Kim, P. S. *Biochemistry* **1990**, *29*, 2891-2894.
(7) Barkhuijsen, H.; de Beer, R.; Bovée, W. M. M. J.; van Ormondt, D. *J. Magn. Reson.* **1985**, *61*, 465-481.
(8) Eisenberg, D.; Weiss, R. M.; Terwilliger, T. C. *Proc. Natl. Acad. Sci. U.S.A.* **1984**, *81*, 140-144.

0002-7863/91/1513-1406$02.50/0